Biochemical Functionalization of Polymeric Cell Substrata Can Alter Mechanical Compliance

M. Todd Thompson,[†,‡] Michael C. Berg,[§] Irene S. Tobias,[†] Jenny A. Lichter,[†] Michael F. Rubner,[†] and Krystyn J. Van Vliet*[,†]

Department of Materials Science and Engineering, Department of Chemical Engineering, and Harvard−MIT Division of Health Sciences and Technology, Massachusetts Institute of Technology, 77 Massachusetts Avenue, Cambridge, Massachusetts 02139

Received February 16, 2006; Revised Manuscript Received April 4, 2006

Biochemical functionalization of surfaces is an increasingly utilized mechanism to promote or inhibit adhesion of cells. To promote mammalian cell adhesion, one common functionalization approach is surface conjugation of adhesion peptide sequences such as Arg-Gly-Asp (RGD), a ligand of transmembrane integrin molecules. It is generally assumed that such functionalization does not alter the local mechanical properties of the functionalized surface, as is important to interpretations of macromolecular mechanotransduction in cells. Here, we examine this assumption systematically, through nanomechanical measurement of the nominal elastic modulus of polymer multilayer films of nanoscale thickness, functionalized with RGD through different processing routes. We find that the method of biochemical functionalization can significantly alter mechanical compliance of polymeric substrata such as weak polyelectrolyte multilayers (PEMs), increasingly utilized materials for such studies. In particular, immersed adsorption of intermediate functionalization reagents significantly decreases compliance of the PEMs considered herein, whereas polymer-on-polymer stamping of these same reagents does not alter compliance of weak PEMs. This finding points to the potential unintended alteration of mechanical properties via surface functionalization and also suggests functionalization methods by which chemical and mechanical properties of cell substrata can be controlled independently.

Introduction

Surface functionalization to promote cellular adhesion to biomaterials used as cellular growth substrata is an important component of many biological research efforts and engineering applications. High-resolution imaging of cytoskeletal substructure and dynamics is critically dependent on the ability to successfully immobilize cells through formation of tight adhesive contacts.[1] In addition, in vitro culture of adherent cell types, whether for tissue engineering or cell biology studies, also depends on the quality and strength of adhesion events.[2−4] In the field of medical implants, precise control of cellular attachment is necessary to prevent microbiological contamination and promote proper graft response, a topic of particular interest in the area of osteogenic implantable devices.[5−7]

Indeed, interfacial biology is a well-developed and rich field, and many types of biointerfacial modifications exist to promote the attachment and proliferation of cells on given synthetic or biomacromolecular growth substrates.[3] Techniques to induce phenotypic change and control spatial distribution in various cell types include alteration of surface topology[8] and/or degree of interchain cross-linking in a polymeric gel,[9] creation of phase-separated amphiphilic surfaces,[10] and functionalization with cell-resistant materials that restrict cell growth and enforce patterning.[11] With increasing frequency, cytophilic surface modifications are employed via adsorption of extracellular matrix proteins or related derivatives onto a rigid or semirigid support to reconstitute aspects of the in vivo extracellular environment. One widely used approach involves the conjugation of proteins or peptides containing the sequence Arg-Gly-Asp (RGD), which recruits and binds to integrin receptors on the surfaces of eukaryotic cells.[3,12−17] This is particularly significant because differential integrin binding alters specific cellular behaviors such as differentiation in human unmbilical vein endothelial cells.[5] Conversely, differential integrin expression is known to be an important marker of cell state during angiogenesis and capillary invasion during wound healing.[18,19]

Increasingly, polyelectrolyte multilayers (PEMs) are used as bioactive substrata for the study of cell adhesion or phenotype.[14,20−26] PEMs are polyelectrolyte complexes fabricated via a layer-by-layer (LbL) assembly process with dilute solutions of positively and negatively charged polymers or by the LbL assembly of weakly interacting hydrogen bond acceptors/donors with polyelectrolyte polymers of complementary polarity. Because the physical properties and film thickness of weak (pH-sensitive) PEMs can be controlled with high precision through assembly conditions such as solution pH, these materials find utility in a range of applications including but not limited to cytophilic substrata and cytophobic coatings. Importantly, these materials effectively modulate cell behavior when assembled to only nanoscale thicknesses,[2] and are thus amenable to high-resolution optical imaging approaches desirable for a range of in vitro cell experiments. Berg et al. have demonstrated that the cytophobic properties of a PEM comprising poly(acrylic acid) (PAA) and polyacrylamide (PAAm) can be reversed via surface functionalization with RGD.[14] In these studies, it is assumed but not demonstrated that biochemical functionalization of such surfaces does not alter the mechanical properties of that surface, such that the mechanical and chemical characteristics of substrata can be modulated independently to evaluate cell response. That is, if surface modifications such as RGD

[†] Department of Materials Science and Engineering.
[‡] Department of Chemical Engineering.
[§] Harvard−MIT Division of Health Sciences and Technology.

10.1021/bm060146b CCC: $33.50
Published on Web 05/06/2006

incorporation alter only the biochemical interface between the substrata and adhered cells, then cellular processes such as adhesion, spreading, proliferation, and differentiation on those surfaces could be attributed unambiguously to biochemical rather than mechanical characteristics of the substrata.

Thompson et al. have shown that mechanical compliance of nanoscale PEM films can be modulated directly via assembly conditions.[2] For weak PEMs comprising PAA and poly(allylamine hydrochloride) or PAH, nominal elastic modulus E varies by orders of magnitude for mod-2 changes in assembly pH, due to the pH-dependent degree of ionic cross-linking that correlates inversely with the capacity to swell in aqueous solutions. Further, Thompson et al. found that this mechanical compliance correlated directly with the capacity of mammalian (microvascular endothelial) cells to attach to and proliferate on unfunctionalized PEMs under in vitro culture, and others have demonstrated similar effects of mechanical compliance for other PEM or hydrogel systems on different adherent mammalian cell types.[21,24,27] Additionally, Picart et al. recently demonstrated that surface functionalization of different PEMs with RGD, with or without intentional chemical cross-linking of the multilayers, could significantly affect the cellular attachment and proliferation of osteoblasts; mechanical compliance was not characterized for any of those PEMs.[28] In light of these previous findings on biochemical and mechanical modulation of cell−substrate adhesion, here we sought to confirm that the mechanical properties of PEMs were unaffected by a particular biochemical surface functionalization process. To that end, we employed scanning probe microscope-enabled nanoindentation to measure the nominal elastic modulus E of PEMs functionalized through various processing routes with a synthetic peptide containing the integrin binding sequence RGD.

Experimental Methods

Materials. Poly(acrylic acid) (PAA) (M_w = 90 000; 25% aqueous solution) and polyacrylamide (PAAm) (M_w = 5 000 000; 1% aqueous solution) were purchased from Polysciences. Poly(allylamine hydrochloride) (PAH) (M_w = 70 000) was purchased from Sigma-Aldrich. Peptides GRGDSPC and GRGESPC were provided by the MIT Biopolymers Lab. Sulfosuccinimidyl 6-[3′-(2-pyridyldithio)propriona-mido]hexanoate (Sulfo-LC−SPDP) was purchased from Pierce Biotechnology. Poly(dimethylsiloxane) (PDMS) stamps were made obtained according to the previously described protocol.[14]

Polymer Multilayer Assembly. Films were assembled as previously described.[14,22,26,29] Briefly, dilute solutions (0.01 M) of PAA, PAAm, and PAH were prepared in deionized water and the solution pH adjusted to 3.0 using HCl. The multilayers were assembled on standard glass slides, silicon wafers, and in 60-mm-diameter polystyrene Petri dishes using an automated layer-by-layer dipping method. Each sample was assembled with one layer of PAH to promote strong adhesion of the PAA/PAAm PEM, followed by 5.5 bilayers of PAA/PAAm. Note that PAA/PAAm multilayers are formed via hydrogen bonding, not ionic cross-linking, at this pH. Thus, the PEMs were then covalently cross-linked, as required for stability at neutral pH conditions required for cell culture, via elevated temperature in a vacuum (180 °C, 2 h for glass and silicon; 90 °C, overnight for polystyrene).

For surface-modified samples, PAH was first added to the surface by one of two routes. In the first case, surface modification was achieved via incubation of the PEM sample in a 0.01 M/pH = 9.0 polyelectrolyte solution at room temperature for 15 min or 30 s (hereafter termed *adsorbed PAH*). In the second case, surface modification was achieved via polymer-on-polymer transfer with a patterned PDMS stamp inked with 0.05 M PAH/pH = 9.0, as described previously (hereafter termed *stamped PAH*).[14] Briefly, PDMS polymer stamps were soaked in a 0.01 M solution of PAH and then allowed to physically contact the PAA/PAAm PEM surface for 30 s before removal. The PEMs were then rinsed with 150 mM/pH = 7.4 phosphate-buffered saline (PBS) several times under agitation and allowed to dry in air for subsequent rehydration and use. Modification of PAH-treated PEMs with RGD or a sequence that does not elicit cell adhesion, Arg-Gly-Glu (RGE), was accomplished first by incubation of 0.5 mM Sulfo-LC−SPDP in the presence of PAH-treated PEMs for 30 min at room temperature. Following the addition of this heterobifunctional cross-linker, the samples were washed with PBS twice for 5 min. Incubation of 0.5 mM peptide solution (GRGDSPC or GRGESPC) in PBS for 8 h at room temperature yielded RGD- and RGE-modified PAA/PAAm samples, ostensibly conjugated to the heterobifunctional cross-linker via a disulfide linkage. PEMs were rinsed several times in PBS under agitation and allowed to dry in air for subsequent rehydration and use.

Mechanical Testing of PAA/PAH Multilayers. Mechanical testing was performed using a scanning probe microscope well-suited for the force−depth acquisition required of nanoindentation (3D Molecular Force Probe or 3DMFP, Asylum Research, Santa Barbara, CA). Commercially available unsharpened silicon nitride cantilevers (MLCT-AUHW, Veeco Metrology Group, Sunnyvale, CA) were used to indent PEMs to maximum depths of ∼20 nm. The probe tip radius of curvature R_p was ∼50 nm, and the cantilever spring constant k was experimentally determined for each cantilever via the thermal power spectral density approach to be within the factory specifications of 0.1 N/m by a factor of 2.[2]

Nanoindentation was performed in an acoustic isolation enclosure (Herzan, Inc.) at room temperature in 0.2-μm-filtered PBS. At least 50 nanoindentation experiments were conducted on each polymer sample, and each indentation was performed at a unique point on the sample surface to rule out effects due to cyclic loading and/or plastic deformation. To ensure that indentation occurred at sites of PAH patterning in PMDS-stamped samples, the sample surface was first imaged in contact mode using the 3DMFP (90 μm × 90 μm), but force−displacement data were not acquired in the same region that was imaged; surface modulation due to contact imaging could thus be neglected in the interpretation of mechanical experiments. Furthermore, multiple regions were tested over a sample area that spanned ∼50% of the total stamped region of the PEM. Finally, multiple samples of the PAH-stamped samples were tested on different days, to identify any sample-to-sample variations and systematic experimental errors.

Nanomechanical Data Analysis. Nanoindentation force−depth data were analyzed in IGOR (Wavemetrics, Lake Oswego, OR) on a windows platform PC using the method previously described.[2] The nominal elastic moduli of the PEM samples were calculated using a spherical Hertzian model of the form

$$P = {}^4/_3 E_r^{1/2} R_p \Delta^{3/2} \quad (1)$$

where P is applied force, E_r is the reduced elastic modulus, R_p is the radius of curvature of the cantilevered probe, and Δ is the depth of penetration into the sample surface.[30]

Force−displacement data were processed prior to analysis using a 25 pass binomial smoothing filter to eliminate random fluctuations.[31] Since accurate determination of the initial contact point is a critical issue in nanoindentation of compliant polymer films,[32,33] an additional noise threshold was applied to the log P − log Δ representation of smoothed curves to identify this (0, 0) point objectively and repeatably. Linear least-squares fits of the log P − log Δ representation of smoothed responses were conducted and yielded intercept values from which nominal E were calculated from eq 1, as previously described.[2]

PEM Film Thickness Measurement. To determine whether any experimentally observed differences in PEM mechanical compliance could be attributed to differences in hydrated film thickness t, separate hydrated samples were assembled on glass substrates and imaged via scanning probe microscopy (SPM) over regions including scratches through the complete sample thickness. Unmodified PAA/PAAm, PAA/PAAm/adsorbed PAH, PAA/PAAm/stamped PAH, and PAA/PAAm/stamped PAH/RGE PEMs of nanoscale thickness were prepared on

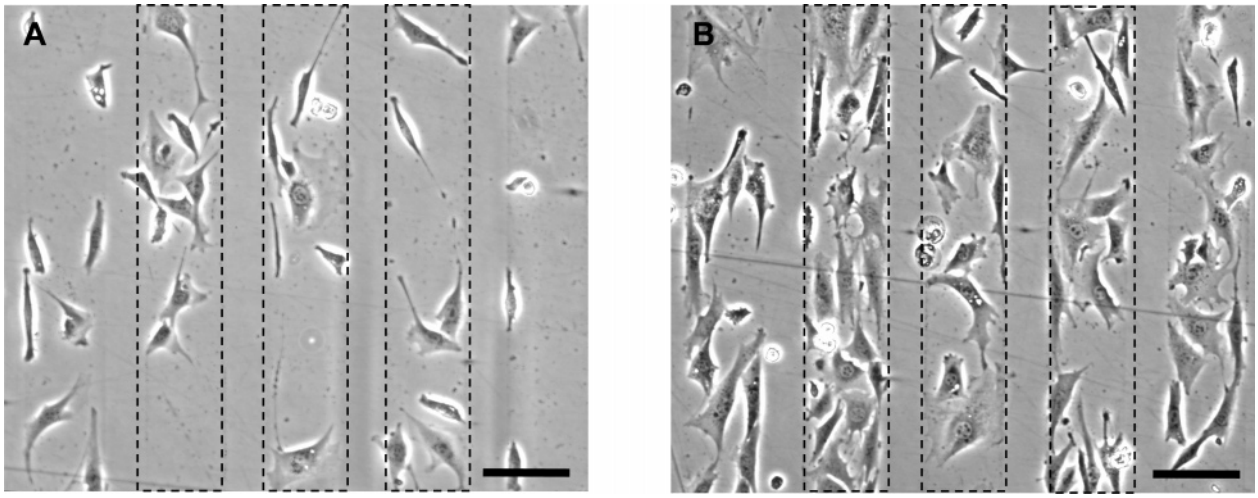

Figure 1. Wild-type NR6 fibroblast attachment as a function of RGD concentration on PAA/PAH PEMs at 48 h postseeding, where the PEM surface was modified via polymer-on-polymer stamping of PAH in a vertical line pattern (dashed rectangles show three representative line widths) followed by RGD conjugation via a heterobifunctional cross-linker. Cells do not adhere as readily on PAA/PAAm PEM lines functionalized with low RGD concentrations of ~53 000 molecules/μm^2 (A), but do adhere readily to the same PAA/PAAm lines functionalized with a higher RGD concentration of 152 000 molecules/μm^2 (B). Scalebars = 50 μm. These materials, cell culture methods, and cell adhesion results are detailed in ref 14.

glass slides as described above. Sample slides were cleaned by dipping in sterile 0.2-μm-filtered PBS, rehydrated in PBS, and scratched with a standard razor blade. PEMs were imaged in contact mode (3DMFP) using a Si_3N_4 probe of $k = 0.06$ N/m over regions including the scratch site at both 0° and 90° scan angles. Height measurements were calculated by measuring ΔZ at six different randomly selected regions, where

$$\Delta Z = Z_{\text{PEM surface}} - Z_{\text{trough}} \quad (2)$$

Standard deviation of the mean sample height was significantly smaller than the associated error in the surface roughness across the trough in individual image cross-sections, which can be attributed to slight damage of the underlying glass substrate and/or limited residual PEM within the scratch trough. Root-mean-square (rms) surface roughness was determined directly from contact images via 3DMFP IGOR subroutines. Average ± standard deviation rms roughness values among six cross-sections within a given sample image are reported. In addition, in situ ellipsometry (ISE) was employed to validate SPM measurements of water-hydrated film thickness t for the same PEMs assembled on silicon substrates. ISE determines t as a function of changes in indices of refraction n measured via light reflected from the material surface and samples square-millimeter-scale surface areas.[22]

Cell Attachment to Modified PEM Substrata. Murine NIH 3T3 fibroblasts were seeded at 40 000 cells/mL onto the following PAA/PAAm (6 bilayer) substrata in triplicate 3.5-cm-diameter wells of tissue culture polystyrene six-well plates (Corning): no further modification (null); 30 s adsorption of PAH (PAH, adsorbed) or 30 s stamp of PAH (PAH, stamped); 30 s adsorption of PAH followed by conjugation of RGD (RGD, PAH adsorbed) or dummy peptide RGE (RGE, PAH adsorbed). Cells were maintained at 37 °C, 5% CO_2, then trypsinized and counted via a hemacytometer as well as calibrated Alamar blue (Biosource) metabolic dye reduction at day 3.

Results and Discussion

Previous studies have demonstrated that, in the absence of surface functionalization with RGD, this PEM substrate is completely cytophobic to both hepatocytes and human microvascular endothelial cells.[2,14] However, using a patterned polymer-on-polymer stamping technique, Berg et al. demonstrated that PAH stamping followed by covalent conjugation of RGD-containing peptides at the multilayer surface could switch the cytophobicity of PAA/PAAm to that of a cytophilic substrate in an RGD concentration-dependent manner (see Figure 1). This response was not reproduced via conjugation of the dummy peptide sequence RGE or by stamping of PAH in the absence of any peptide sequence and thus attributed to specific chemical interactions between this particular adhesive ligand and the mammalian cell surfaces.[14]

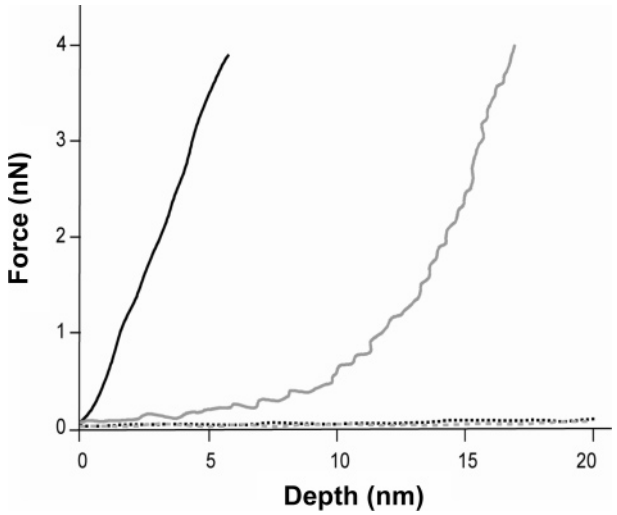

Figure 2. Representative force−depth responses acquired during nanoindentation of PAA/PAAm PEMs in 150 mM phosphate-buffered saline: PAA/PAAm/adsorbed PAH, 15 min (solid black); PAA/PAAm/adsorbed PAH + RGD (solid gray); unmodified PAA/PAAm (dashed black); PAA/PAAm/stamped PAH, 30 s (dashed gray).

Effect of Surface Functionalization on Mechanical Compliance. To ascertain any changes in mechanical properties of these PEMs that such surface engineering may engender, instrumented nanoindentation was performed on samples representing each processing step during surface modification of PAA/PAAm with RGD or RGE. Representative $P - \Delta$ responses for each PEM sample are shown in Figure 2, and nominal elastic moduli E calculated from such data are shown as a function of surface modification in Figure 3. The unmodified PEM exhibits a nominal E (2.4×10^5 Pa), consistent with the high swelling capacity and low cross-linking density of this PEM, as well as with previous mechanical analysis of this

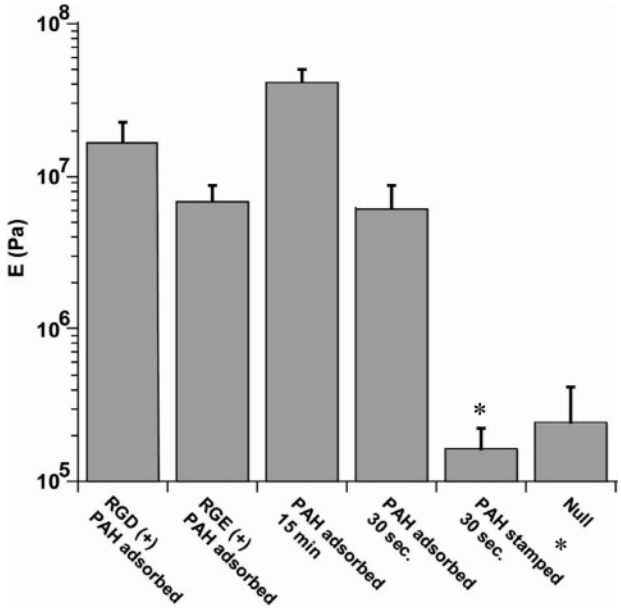

Figure 3. Nominal elastic moduli *E* as measured by instrumented nanoindentation of surface-modified PAA/PAAm polymer multilayers. PEMs were indented to a depth of 20 nm using a scanning probe microscope in fluid (150 mM PBS, pH = 7.4) at room temperature. Error bars represent standard deviation among at least 50 measurements on a single sample, and * indicates statistically significant differences of $p < 0.05$ (ANOVA).

polymer film.[2,14,26,34] The second step in the process of surface engineering involves the addition of PAH as a base for conjugation of RGD. This can be readily accomplished by adsorption of the polymer chain from a dilute solution of PAH or by polymer-on-polymer stamping as described by Berg et al.[14] Samples prepared with PAH according to this stamping protocol exhibited a slightly lower mean *E* with respect to the unmodified PEM (1.6×10^5 Pa); this difference was found to be within the margin of error of the nanoindentation approach. Although it is possible that subsequent conjugation of stamped PAH could unintentionally alter mechanical stiffness, it is unlikely that *E* would substantially increase. Indeed, *adsorbed* PAH samples that were subsequently conjugated with RGD/RGE showed a decrease in elastic modulus relative to samples where PAH was adsorbed without subsequent conjugation (Figure 3.) Therefore, one may reasonably conclude that PAA/PAAm multilayers modified via *stamped PAH* and RGD conjugation reverse the reported cytophobicity of this multilayer[2] due chiefly to changes in RGD ligand concentration, and not to unintended changes in mechanical compliance of the polymer substrata.

In contrast, PEMs modified by *adsorbed PAH* (15 min) exhibited $E = 4.16 \times 10^7$ Pa, an increase in mechanical stiffness by more than 2 orders of magnitude. PEMs modified via adsorbed PAH followed by either RGD or RGE peptide conjugation showed similar, dramatic increases in stiffness ($E = 1.67 \times 10^7$ Pa and 6.74×10^6 Pa, respectively) with respect to the unmodified PEM or the stamped PAH modification. Therefore, it is demonstrated that the transition from a mechanically compliant PEM to a mechanically stiff PEM occurs at the point of PAH adsorption, and not through the addition of the Sulfo-LC-SPDP heterobifunctional cross-linker or the RGD/RGE heptamers. Reducing the PAH incubation time to 30 s, the time the time scale of PDMS stamping, showed only a modest reduction in the stiffness ($E = 6.15 \times 10^6$ Pa), suggesting that this material modification occurs rapidly.

Table 1. Properties of PAA/PAAm Polymer Multilayer Derivatives[a]

sample	PAA/PAAm bilayers	hydrated thickness [nm]	surface roughness [nm]	E [10^5 Pa]
PAA/PAAm, RGD modified[b]	5.5			167.0 ± 60.0
PAA/PAAm, RGE modified[b]	5.5	214.2 ± 48.0	94.5 ± 69.6	67.4 ± 19.9
PAA/PAAm, PAH adsorbed[c]	5.5	99.8 ± 16.6	52.0 ± 37.8	416.0 ± 89.2
PAA/PAAm, PAH stamped[d]	5.5	213.1 ± 59.5	130.2 ± 95.7	15.9 ± 0.6
PAA/PAAm (null; no PAH)	5.0	87.8 ± 19.3	34.1 ± 23.5	2.4 ± 1.7

[a] Young's moduli *E* were measured via nanoindentation. Hydrated thickness and surface roughness were acquired separately through scanning probe microscopy imaging of a surface area including a scratch through the complete sample thickness. [b] PAH adsorbed for 15 min, followed by Sulfo-LC-SPDP and RGD or RGE heptamer, as indicated. RGD-modified samples were not analyzed for hydrated thickness and surface roughness to conserve peptide, but the difference of only one methylene unit between the RGD and RGE amino acid sidechains would not be predictive of any differences between these samples. [c] PAH adsorbed for 15 min. Figure 2 demonstrates no significant effect of shorter (30 s) adsorption duration on *E*. [d] PAH stamped for 30 s.

Consideration of PEM Film Thickness. It is not immediately apparent why the compliance of PAA/PAAm/adsorbed PAH PEMs is so dramatically affected by adsorption of the PAH polycation. One possible explanation is that the sample thickness decreases significantly after adsorption of PAH (e.g., by increased interchain hydrated cross-linking), such that mechanical probing of all samples to the same depth ($\Delta \approx 20$ nm) induces artifacts associated with proximity to the rigid polystyrene substrate on which the PEMs were assembled. To address this possibility, PEM film thickness was determined via scanning probe microscopy contact-mode imaging for all samples. As shown in Table 1, surface modifications did not significantly decrease PEM thickness. In fact, the nanoscale thickness and rms surface roughness of PAA/PAAm with an adsorbed layer of PAH was slightly greater than that of unmodified PAA/PAAm (null), which is consistent with the increased deposition of more material in the modified film. Similarly, PAA/PAAm with an adsorbed layer of PAH conjugated with a heterobifunctional cross-linker and capped with RGE−peptide showed an increase in thickness and rms surface roughness consistent with greater material deposition. PAA/PAAm samples modified by polymer-on-polymer stamping of PAH alone exhibited a thickness comparable to the RGE-modified surfaces with similar increases in the rms surface roughness. This is possibly due to the inhomogeneous nature of the polymer-on-polymer stamping technique, and also because PAH deposited in this localized fashion is not free to distribute uniformly and reorient optimally across the PEM surface over the time scale of the stamping procedure. In situ ellipsometry (ISE) results for the same PEMs assembled on silicon and hydrated with water were consistent with these SPM measurements of hydrated film thickness *t* and are representative of a much larger surface area than considered via SPM. Hydrated *t* of unmodified and adsorbed PAH PEMs measured via ISE was ~100 nm, and that of stamped PAH PEMs with and without RGE heptamer was ~230 nm.

Thus, the observed change in *E* between unmodified PAA/PAAm and the associated PAH adsorbed derivative cannot be attributed to a significant decrease in sample thickness upon PAH adsorption. Although differences in apparent *t* as measured via AFM are noted when comparing PEMs functionalized via adsorbed PAH (15 min) to stamped PAH, the effective strain expressed as the ratio of indentation depth ($\Delta = 20$ nm) to film thickness *t* was less than 20% in both cases, and thus, artifacts

due to contributions of the underlying (polystyrene) substrate are minimal.[35] In addition, adsorbed PAH/RGE-conjugated PEMs of thickness nearly identical to that of the stamped PAH PEMs showed significantly decreased compliance that cannot be attributed to differences in PEM thickness.

Neither the amount of total PAH adsorbed onto the surface nor the amount of PAH transferred via stamping were quantified rigorously. Therefore, it remains possible that observed increases in the *E* upon PAH adsorption are related to differences in the amount of PAH integrated within the PEM surface in each deposition protocol, even for constant duration of PAH exposure (30 s). As the PAH was added at a basic pH (pH = 9.0), it is possible that the single bilayer of PAA/PAH assembled at this pH creates a mechanically stiff surface layer.[2] However, the depth of indentation chosen herein (20 nm) exceeds that of a hydrated bilayer by more than an order of magnitude, so such a surface-confined effect would not be expected to elicit the dramatic changes in *E* observed in Figure 3. Therefore, even if the effective concentration of PAH available to react with the underlying PAA/PAAm PEM was greater under adsorption conditions than under stamped conditions, the increase in stiffness of the PAA/PAAm PEMs modified by adsorbed PAH cannot be easily explained by the formation of a mechanically stiff PAA/PAH layer at the PEM surface. Some groups have reported that multilayers are capable of complete exchange of either the polycation or the polyanion with soluble polyelectrolytes of like charge introduced postassembly under certain conditions.[36−38] Moreover, it has shown that a liquidlike state exists where PEMs dissolve and either equilibrate to new, more stable configurations or disassemble entirely.[39,40] When taken together, such results might suggest that the polymer multilayer is undergoing a reconstitution during the adsorptive addition of PAH. However, the PAA/PAAm films in this study are covalently cross-linked via elevated temperature postassembly, so it is unlikely that there is dissolution or complete exchange of PAAm with PAH during the 15 min incubation time. Additionally, a 30 s incubation time for PAH adsorption still produces a dramatic change in the modulus relative to the unmodified PEM ($E = 6.15 \times 10^6$ Pa and 1.6×10^5 Pa, respectively), which is more rapid than the exchange processes reported thus far. Also, the PAH adsorption steps were performed under relatively mild conditions with respect to temperature and pH, whereas previous studies required modulation of pH, temperature, or ionic strength to achieve exchange and/or dissolution of PEMs.[36−40] However, it is possible that this adsorption step induced potential phase transitions/separations, which would be consistent with the observed slight increase in opacity of the PEM upon PAH adsorption, and this possible phase transition is currently under investigation. The central finding remains clear: Mechanical properties of weak PEMs can be significantly and unintentionally altered via certain biochemical surface modification routes, and these effects are independent of PEM thickness.

Effect of Surface Functionalization on Cell Attachment. Previous results in several substrata material systems have indicated that the mechanical stiffness of a polymeric substrate can affect cell attachment, spreading, and proliferation. As we observed decreased mechanical compliance in these PEMs upon the adsorption of PAH, we explored whether cell attachment correlated more strongly with compliance or with adhesive peptide functionalization. In triplicate, murine NIH 3T3 fibroblasts were seeded onto PEM substrata to which PAH had been either adsorbed for 30 s or stamped for 30 s, with or without subsequent addition of the adhesive ligand RGD or the dummy (anti-adhesive) peptide RGE; total cell number at day 3 was measured upon trypsinization. As shown in Figure 4, cells attached as a function of both substrata compliance and surface functionalization. For example, RGD-functionalized, stiff substrata (RGD, PAH-adsorbed) showed significantly greater cell attachment than RGD-functionalized, compliant substrata (RGD, PAH-stamped). However, the RGD-functionalized, compliant substrata (RGD, PAH-stamped) showed nearly the same number of cells per square centimeter attached as the unfunctionalized, stiff substrata (PAH-adsorbed); and the anti-adhesive peptide RGE-functionalized, stiff substrata (RGE, PAH-adsorbed) showed nearly the same cell attachment as unfunctionalized, stiff substrata (PAH-adsorbed). Taken together, these results suggest that the mechanical compliance of the underlying cell substrata can be at least as important as ligand functionalization in dictating efficient cell attachment and proliferation.

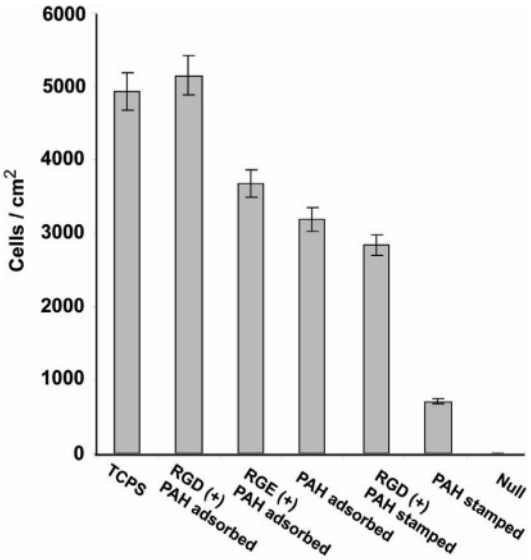

Figure 4. Murine NIH 3T3 fibroblast attachment at day 3 as a function of surface functionalization, expressed in units of functionalized surface area (mean +/− standard deviation). TCPS is tissue culture polystyrene; surface functionalization of PAA/PAAm (null) as indicated in Table 1. Growth area for stamped samples is 0.25 μm^2, whereas growth area for all other samples is 9.6 μm^2.

Conclusions

Biochemical surface modification of polymeric growth substrates to enhance or inhibit cellular attachment is important for a wide range of biological and bioengineering problems. Typically, it is tacitly assumed that these modifications—including incorporation of adhesion proteins and peptides such as RGD—alter only the local chemical environment and leave the mechanical properties of the surface unaffected. Here, the effect of RGD incorporation on the mechanical compliance of a specific polymer multilayer system comprising poly(acrylic acid) and polyacrylamide has been characterized systematically. Significant processing-dependent changes in nominal elastic modulus *E* have been demonstrated: For the weak PEM considered herein, surface functionalization with RGD via polymer-on-polymer stamping of dilute PAH does not alter mechanical compliance, whereas functionalization via adsorption of dilute PAH over the same duration dramatically increases *E*. Thus, for weak polymer multilayers of nanoscale thickness such as PAA/PAAm, the method by which the cellular interface is modified can have unintended and profound consequences on mechanical compliance of the substrata and thereby alter

the mechanical environment of attached cells. Furthermore, the changes in substratum mechanical compliance demonstrated herein cannot be attributed to changes in sample thickness or surface roughness. It is an open and important question whether these results are generally true for other polyelectrolyte multilayer systems and/or polymeric hydrogels. These findings serve both as a caution in the design of surfaces and experiments for which only chemical modification is desired and as an opportunity to choose surface modification routes that alter mechanical and biochemical interfaces independently.

Acknowledgment. M. T. Thompson and K. J. Van Vliet acknowledge use of the 3DMFP (Asylum Research, Inc.) within the MIT Department of Materials Science and Engineering Nanomechanical Technology Laboratory. J. A. Lichter and M. C. Berg acknowledge use of shared experimental facilities in the Institute for Soldier Nanotechnologies. M. T. Thompson acknowledges support through the National Institutes of Health Bioinformatics and Integrative Genomics Training Grant. This work was supported in part by and made use of the Shared Experimental Facilities supported by the MRSEC Program of the National Science Foundation under award number DMR 02-13282.

References and Notes

(1) Linder, A.; Weiland, U.; Apell, H. J. *J. Struct. Biol.* **1999**, *126* (1), 16−26.
(2) Thompson, M. T.; Berg, M. C.; Tobias, I. S.; Rubner, M. F.; Van Vliet, K. J. *Biomaterials* **2005**, 26, 6836−45.
(3) McGregor, W. C. *Interfacial Phenomena and Bioproducts*; Marcel Dekker, Inc.: Madison, 1996; Vol. 23, p 510.
(4) Lee, K. Y.; Mooney, D. J. *Chem. Rev.* **2001**, *101* (7), 1869−1879.
(5) Keselowsky, B. G.; Collard, D. M.; Garcia, A. J. *Proc. Natl. Acad. Sci. U.S.A.* **2005**, *102* (17), 5953−7.
(6) Liao, H.; Andersson, A. S.; Sutherland, D.; Petronis, S.; Kasemo, B.; Thomsen, P. *Biomaterials* **2003**, *24* (4), 649−54.
(7) Ignatius, A.; Peraus, M.; Schorlemmer, S.; Augat, P.; Burger, W.; Leyen, S.; Claes, L. *Biomaterials* **2005**, *26* (15), 2325−32.
(8) Andersson, A. S.; Backhed, F.; von Euler, A.; Richter-Dahlfors, A.; Sutherland, D.; Kasemo, B. *Biomaterials* **2003**, *24* (20), 3427−36.
(9) Pelham, R. J.; Wang, Y. L. *Proc. Natl. Acad. Sci. U.S.A.* **1997**, *94* (25), 13661−13665.
(10) Rimmer, S.; German, M. J.; Maughan, J.; Sun, Y.; Fullwood, N.; Ebdon, J.; MacNeil, S. *Biomaterials* **2005**, *26* (15), 2219−30.
(11) Kumar, G.; Wang, C. W.; Co, C.; Ho, C. *Langmuir* **2003**, *19* (25), 10550−10556.
(12) Hersel, U.; Dahmen, C.; Kessler, H. *Biomaterials* **2003**, *24* (24), 4385−415.
(13) Gailit, J.; Clarke, C.; Newman, D.; Tonnesen, M. G.; Mosesson, M. W.; Clark, R. A. *Exp. Cell Res.* **1997**, *232* (1), 118−26.
(14) Berg, M. C.; Yang, S. Y.; Hammond, P. T.; Rubner, M. F. *Langmuir* **2004**, *20* (4), 1362−1368.
(15) Lieb, E.; Hacker, M.; Tessmar, J.; Kunz-Schughart, L. A.; Fiedler, J.; Dahmen, C.; Hersel, U.; Kessler, H.; Schulz, M. B.; Gopferich, A. *Biomaterials* **2005**, *26* (15), 2333−41.
(16) Holland, J.; Hersh, L.; Bryhan, M.; Onyiriuka, E.; Ziegler, L. *Biomaterials* **1996**, *17* (22), 2147−56.
(17) Drumheller, P. D.; Hubbell, J. A. *Anal. Biochem.* **1994**, *222* (2), 380−8.
(18) Gailit, J.; Clark, R. A. *Curr. Opin. Cell Biol.* ***1994***, 6 (5), 717−25.
(19) Feng, X.; Clark, R. A.; Galanakis, D.; Tonnesen, M. G. *J. Invest. Dermatol.* **1999**, *113* (6), 913−9.
(20) Boura, C.; Muller, S.; Vautier, D.; Dumas, D.; Schaaf, P.; Voegel, J. C.; Stoltz, J. F.; Menu, P. *Biomaterials* **2005**, *26*, 4568−4575.
(21) Engler, A. J.; Richert, L.; Wong, J. Y.; Picart, C.; Discher, D. E. *Surf. Sci.* **2004**, *570*, 142−154.
(22) Mendelsohn, J. D.; Yang, S. Y.; Hiller, J.; Hochbaum, A. I.; Rubner, M. F. *Biomacromolecules* **2003**, *4* (1), 96−106.
(23) Ngankam, A.; Mao, G.; Tassel, P. V. *Langmuir* **2004**, *20*, 3362−3370.
(24) Richert, L.; Engler, A. J.; Discher, D. E.; Picart, C. *Biomacromolecules* **2004**, *5* (5), 1908−16.
(25) Salloum, D.; Olenych, S.; Keller, T.; Schlenoff, J. *Biomacromolecules* **2005**, *6*, 161−167.
(26) Yang, S. Y.; Mendelsohn, J. D.; Rubner, M. F. *Biomacromolecules* **2003**, *4* (4), 987−994.
(27) Brown, X.; Ookawa, K.; Wong, J. *Biomaterials* **2005**, *26*, 3123−3129.
(28) Picart, C.; Elkaim, R.; Richert, L.; Audoin, T.; Arntz, Y.; Cardoso, M. D.; Schaaf, P.; Voegel, J. C.; Frisch, B. *Adv. Funct. Mater.* **2005**, *15* (1), 83−94.
(29) Yang, S. Y.; Rubner, M. F. *J. Am. Chem. Soc.* **2002**, *124* (10), 2100−2101.
(30) Johnson, K. L. *Contact Mechanics*; Cambridge University Press: Cambridge, 1994;
(31) Marchand, P.; Marmet, L. *Rev. Sci. Instrum.* **1983**, *54* (8), 1034−1041.
(32) Dimitriadis, E.; Horkay, F.; Maresca, J.; Kachar, B.; Chadwick, R. *Biophys. J.* **2002**, *82*, 2798−2810.
(33) Domke, J.; Radmacher, M. *Langmuir* **1998**, *14* (12), 3320−3325.
(34) Yang, S. Y.; Berg, M. C.; Hammond, P. T.; Rubner, M. F. In *Primary hepatocytes and fibroblasts response to polyelectrolyte multilayers with polyacrylamide containing polymers*; American Chemical Society: Washington, DC, 2003.
(35) Oommen, B.; Van Vliet, K. J. *Thin Solid Films* In press and available online.
(36) Ball, V.; Hubsch, E.; Schweiss, R.; Voegel, J. C.; Schaaf, P.; Knoll, W. *Langmuir* **2005**, *21* (18), 8526−31.
(37) Boulmedais, F.; Bozonnet, M.; Schwinte, P.; Voegel, J. C.; Schaaf, P. *Langmuir* **2003**, *19* (23), 9873−9882.
(38) Jomaa, H. W.; Schlenoff, J. B. *Langmuir* **2005**, *21* (18), 8081−4.
(39) Kovacevic, D.; van der Burgh, S.; de Keizer, A.; Stuart, M. A. C. *Langmuir* **2002**, *18* (14), 5607−5612.
(40) Kovacevic, D.; van der Burgh, S.; de Keizer, A.; Stuart, M. A. C. *J. Phys. Chem. B* **2003**, *107* (32), 7998−8002.

BM060146B